Practical phase unwrapping of interferometric fringes based on unscented Kalman filter technique

Zhongtao Cheng,[1] Dong Liu,[1,*] Yongying Yang,[1] Tong Ling,[1] Xiaoyu Chen,[1] Lei Zhang,[1] Jian Bai,[1] Yibing Shen,[1] Liang Miao,[2] and Wei Huang[2]

[1]*State Key Lab. Of Modern Optical Instrumentation, College of Optical Science and Engineering, Zhejiang University, Hangzhou, Zhejiang 310027, China*

[2]*State Key Laboratory of Applied Optics, Changchun Institute of Optics, Fine Mechanics and Physics, Chinese Academy of Sciences, Changchun, Jilin 130033,China*

[*]*liudongopt@zju.edu.cn*

Abstract: A phase unwrapping algorithm for interferometric fringes based on the unscented Kalman filter (UKF) technique is proposed. The algorithm can bring about accurate phase unwrapping and good noise suppression simultaneously by incorporating the true phase and its derivative in the state vector estimation through the UKF process. Simulations indicate that the proposed algorithm has better accuracy than some widely employed phase unwrapping approaches in the same noise condition. Also, the time consumption of the algorithm is reasonably acceptable. Applications of the algorithm in our different optical interferometer systems are provided to demonstrate its practicability with good performance. We hope this algorithm can be a practical approach that can help to reduce the systematic errors significantly induced by phase unwrapping process for interferometric measurements such as wavefront distortion testing, surface figure testing of optics, etc.

OCIS codes: (100.5088) Phase unwrapping; (120.3180) Interferometry; (120.5050) Phase measurement.

References and links

1. L. Zhang, C. Tian, D. Liu, T. Shi, Y. Yang, H. Wu, and Y. Shen, "Non-null annular subaperture stitching interferometry for steep aspheric measurement," Appl. Opt. **53**(25), 5755–5762 (2014).
2. D. Liu, Y. Yang, L. Wang, and Y. Zhuo, "Real time diagnosis of transient pulse laser with high repetition by radial shearing interferometer," Appl. Opt. **46**(34), 8305–8314 (2007).
3. D. Malacara, *Optical Shop Testing*, (Wiley, 2007).
4. J. H. Bruning, D. R. Herriott, J. E. Gallagher, D. P. Rosenfeld, A. D. White, and D. J. Brangaccio, "Digital Wavefront Measuring Interferometer for Testing Optical Surfaces and Lenses," Appl. Opt. **13**(11), 2693–2703 (1974).
5. M. Takeda, H. Ina, and S. Kobayashi, "Fourier-transform method of fringe-pattern analysis for computer-based topography and interferometry," J. Opt. Soc. Am. **72**(1), 156–160 (1982).
6. D. C. Ghiglia. and M. D. Pritt, *Two-Dimensional Phase Unwrapping:Theory, Algorithm, and Software*,(Wiley, 1990).
7. R. M. Goldstein, H. A. Zebker, and C. L. Werner, "Satellite radar interferometry: Two-dimensional phase unwrapping," Radio Sci. **23**(4), 713–720 (1988).
8. H. Zhong, J. Tang, and S. Zhang, "Phase quality map based on local multi-unwrapped results for two-dimensional phase unwrapping," Appl. Opt. **54**(4), 739–745 (2015).
9. D. J. Bone, "Fourier fringe analysis: the two-dimensional phase unwrapping problem," Appl. Opt. **30**(25), 3627–3632 (1991).
10. T. J. Flynn, "Consistent 2-D phase unwrapping guided by a quality map," in *Proceedings of the 1996 International Geoscience and Remote Sensing Symposium. Part 3 (of 4), May 28, 1996 - May 31, 1996*(IEEE, Lincoln, NE, USA, 1996), pp. 2057–2059.
11. D. C. Ghiglia and L. A. Romero, "Robust two-dimensional weighted and unweighted phase unwrapping that uses fast transforms and iterative methods," J. Opt. Soc. Am. A **11**(1), 107–117 (1994).

#251481 Received 9 Oct 2015; revised 19 Nov 2015; accepted 19 Nov 2015; published 8 Dec 2015

12. M. Servin, F. J. Cuevas, D. Malacara, J. L. Marroquin, and R. Rodriguez-Vera, "Phase unwrapping through demodulation by use of the regularized phase-tracking technique," Appl. Opt. **38**(10), 1934–1941 (1999).
13. C. Tian, Y. Yang, D. Liu, Y. Luo, and Y. Zhuo, "Demodulation of a single complex fringe interferogram with a path-independent regularized phase-tracking technique," Appl. Opt. **49**(2), 170–179 (2010).
14. J. C. Estrada, M. Servin, and J. A. Quiroga, "Noise robust linear dynamic system for phase unwrapping and smoothing," Opt. Express **19**(6), 5126–5133 (2011).
15. M. A. Navarro, J. C. Estrada, M. Servin, J. A. Quiroga, and J. Vargas, "Fast two-dimensional simultaneous phase unwrapping and low-pass filtering," Opt. Express **20**(3), 2556–2561 (2012).
16. J. C. Estrada, M. Servin, and J. Vargas, "2D simultaneous phase unwrapping and filtering: A review and comparison," Opt. Lasers Eng. **50**(8), 1026–1029 (2012).
17. O. Loffeld, H. Nies, S. Knedlik, and W. Yu, "Phase unwrapping for SAR interferometry - A data fusion approach by Kalman filtering," IEEE Trans. Geosci. Rem. Sens. **46**(1), 47–58 (2008).
18. R. Kulkarni and P. Rastogi, "Phase derivative estimation from a single interferogram using a Kalman smoothing algorithm," Opt. Lett. **40**(16), 3794–3797 (2015).
19. X. Xie and Y. Li, "Enhanced phase unwrapping algorithm based on unscented Kalman filter, enhanced phase gradient estimator, and path-following strategy," Appl. Opt. **53**(18), 4049–4060 (2014).
20. L. Tao, Z. Liu, W. Zhang, and Y. Zhou, "Frequency-scanning interferometry for dynamic absolute distance measurement using Kalman filter," Opt. Lett. **39**(24), 6997–7000 (2014).
21. X. Xianming and P. Yiming, "Multi-baseline phase unwrapping algorithm based on the unscented Kalman filter," IET Radar Sonar Navig. **5**(3), 296–304 (2011).
22. T. E. Zander, V. Madyastha, A. Patil, P. Rastogi, and L. M. Reindl, "Phase-step estimation in interferometry via an unscented Kalman filter," Opt. Lett. **34**(9), 1396–1398 (2009).
23. I. P. Gurov and A. S. Zakharov, "Analysis of characteristics of interference fringes by nonlinear Kalman filtering," Opt. Spectrosc. **96**(2), 175–181 (2004).
24. I. Gurov, E. Ermolaeva, and A. Zakharov, "Analysis of low-coherence interference fringes by the Kalman filtering method," J. Opt. Soc. Am. A **21**(2), 242–251 (2004).
25. S. J. Julier and J. K. Uhlmann, "Unscented filtering and nonlinear estimation," Proc. IEEE **92**(3), 401–422 (2004).
26. Z. Cheng, D. Liu, J. Luo, Y. Yang, Y. Zhou, Y. Zhang, L. Duan, L. Su, L. Yang, Y. Shen, K. Wang, and J. Bai, "Field-widened Michelson interferometer for spectral discrimination in high-spectral-resolution lidar: theoretical framework," Opt. Express **23**(9), 12117–12134 (2015).
27. X. Chen, Y. Yang, C. Wang, D. Liu, J. Bai, and Y. Shen, "Aberration calibration in high-NA spherical surfaces measurement on point diffraction interferometry," Appl. Opt. **54**(13), 3877–3885 (2015).
28. D. Wang, Y. Yang, C. Chen, and Y. Zhuo, "Point diffraction interferometer with adjustable fringe contrast for testing spherical surfaces," Appl. Opt. **50**(16), 2342–2348 (2011).
29. T. Ling, D. Liu, Y. Yang, L. Sun, C. Tian, and Y. Shen, "Off-axis cyclic radial shearing interferometer for measurement of centrally blocked transient wavefront," Opt. Lett. **38**(14), 2493–2495 (2013).

1. Introduction

Interferometric measurement plays an important role in sensing various physical properties such as surface deformation of optics [1], wavefront distortion [2], and so on [3]. In optical interferometry, most techniques, for example, phase-shifting method [4], spatial carrier method [5], etc., give the wrapped demodulated phase. To retrieve the true physical properties, the wrapped phase needs to be further unwrapped in order to yield a continuous phase map. Ideally, the unwrapping problem is trivial for phase maps with good quality where the signal is free of noise. In realistic conditions, however, the phase unwrapping would be of low precision or even fail when the phase map is corrupted by serious noise or there exists phase aliasing [6]. Thus, researchers show intensive interests in this topic and many ingenious algorithms have been developed to perform practical phase unwrapping. We can generally divide these existing phase unwrapping algorithms into three categories. The first are those path-following algorithms, in which the unwrapping process starts from a grid point and integrates the wrapped phase differences following a pre-chosen path [7–10]. Although the path-following algorithms work well for many cases, it is not stable enough because the detected phase discontinuity or residue points which are used to generate the unwrapping path would be affected by the high noise condition easily. The second type are in the framework of minimum-norm, which seek the unwrapped phase whose local derivatives match the measured derivatives as closely as possible [11]. However, the residual unwrapping error of the minimum-norm method is relatively large sometimes. The third type of phase unwrapping algorithms are featured with filtering the phase noise and unwrapping the phase

#251481 Received 9 Oct 2015; revised 19 Nov 2015; accepted 19 Nov 2015; published 8 Dec 2015

simultaneously, such as the regularized phase-tracking (RPT) phase unwrapping approach [12, 13], the recursive phase unwrapping (RPU) system [14–16], the extended Kalman filtering phase unwrapping (EKFPU) algorithm [17], etc. It is considered that separated filtering and unwrapping processes may impair the phase information irreversibly to some extent, thus this type of phase unwrapping algorithms can provide accurate and reasonable noise-immune unwrapping.

The Kalman filter (KF) based techniques have already been extensively used in the signal processing realm. Since it can perform optimal estimations for desirable quantities with good noise immunity, they also attract many interests in different interferometric applications nowadays [17–24]. However, the original KF can only deal with linear problems, and is not appropriate for the non-linear phase unwrapping. The extended Kalman filtering (EKF) is a variant of the original KF, which adopts linear approximation to the nonlinear problem. Although the EKF has already been used to unwrap the interference phase maps as mentioned above, the linear approximation process limits the further promotion of unwrapping accuracy and sometimes induces algorithm divergence. As an improved version of the EKF, the unscented Kalman filter (UKF) introduces the unscented transformation to analyze the statistical features of the prediction and correction processes [25], thus it does not require any linear approximation to the estimation problem. As of today, few works are done to introduce the UKF technique into the application of phase unwrapping except the relevant studies in [19, 21], to our knowledge.

In this paper, we add a new contribution to the phase unwrapping solution for interferometric fringes based on the UKF technique. The proposed algorithm involves the true phase and its derivative simultaneously in the state vector estimation through the UKF process, thus no other assistant local gradient estimator for the phase map is needed, which makes for simple algorithm realization and high computation efficiency. Also, the path-following strategy is unnecessary. We demonstrate that the proposed approach has good noise-immune ability and unwrapping accuracy as well as reasonably acceptable computation consumption compared to some widely employed phase unwrapping algorithms. This algorithm is expected to be a practical choice for the interferometric measurement, such as surface figure testing, wavefront distortion testing, etc., to enhance the accuracy during the data processing.

2. Proposed phase unwrapping algorithm

2.1 Principle and methodology

The phase unwrapping problem assumes that the modulo 2π phase can be obtained, which is very easy to be satisfied in the phase-shift interferometers and spatial-carrier interferometers by converting the arctangent principal value into 2π interval. The wrapped phase can be represented equivalently by its cosine and sine terms:

$$\begin{cases} C(x,y) = \cos(\phi_{2\pi}) \\ S(x,y) = \sin(\phi_{2\pi}) \end{cases}, \tag{1}$$

where, $\phi_{2\pi}$ is the wrapped modulo 2π phase. The proposed algorithm unwraps the phase by seeking for a smooth and continuous phase map that can produce the same cosine and sine results as calculated from Eq. (1), which seems to be a little bit similar with the essence of the RPT technique [12]. It should be noted that, the proposed approach would also be potential to process the phase retrieval of one real fringe pattern if some other techniques such as the Hilbert transformation can be combined to produce the sine term in Eq. (1). In this paper, we mainly concentrate on the phase unwrapping problem.

#251481 Received 9 Oct 2015; revised 19 Nov 2015; accepted 19 Nov 2015; published 8 Dec 2015

Assume that the true phase at an unwrapped pixel, $\phi(k)$, is differentiable, where, k is the pixel index according to some unwrapping strategy as will be introduced below. In most interferometric measurements, this assumption is acceptable because the phase maps correspond to continuous physical quantities. Then, we can infer the true phase value at its adjacent pixel $\phi(k+1)$ from $\phi(k)$ based on the one-order Taylor series expansion model:

$$\phi(k+1)=\phi(k)+\phi'(k)\cdot\Delta k. \tag{2}$$

where, Δk is the discretization step which is one pixel here. If the state vector of the state-space dynamic model for the phase unwrapping problem is defined as $\mathbf{x}_k=\left[\phi(k)\quad \phi'(k)\right]^T$, the true state vector $\mathbf{x}_{k+1}$ at the pixel $k+1$ can also be evolved from the value $\mathbf{x}_k$ according to Eq. (2):

$$\mathbf{x}_{k+1}=f\left(\mathbf{x}_k,\mathbf{v}_k\right)=\mathbf{F}\mathbf{x}_k+\mathbf{v}_k, \tag{3}$$

where,

$$\mathbf{F}=\begin{bmatrix}1 & 1\\ 0 & 1\end{bmatrix}, \tag{4}$$

and $\mathbf{v}_k$ is the process error vector using the one-order approximation of Eq. (2). We emphasize that, different from the commonly used random walk model in KF technique [19, 21], the state-space model of Eq. (3) involves the true phase and its derivative into the state vector estimation. Thus, no other phase derivative estimator is needed, making the phase unwrapping much simpler.

The observation equation is

$$\mathbf{y}_k=h\left(\mathbf{x}_k,\mathbf{n}_k\right)=H\left(\mathbf{x}_k\right)+\mathbf{n}_k. \tag{5}$$

Herein, $\mathbf{y}_k$ represents the observation vector whose elements are the cosine term and sine term from Eq. (1), $\mathbf{n}_k$ is the observation noise vector, and the operator H is defined as

$$H\left(\mathbf{x}\right)=\begin{bmatrix}C(k)\\ S(k)\end{bmatrix}=\begin{bmatrix}\cos(x_1)\\ \sin(x_1)\end{bmatrix}, \tag{6}$$

where, x_1 denotes the first element in the state vector $\mathbf{x}$.

Based on the state-space equation [Eq. (3)] and the observation equation [Eq. (5)], the UKF technique can be employed to unwrap the whole phase map pixel-by-pixel through combining the model predicted cosine and sine terms and their real observations to produce an optimal estimation for the desirable state vector. Note that, the elements in noise vectors $\mathbf{v}_k$ and $\mathbf{n}_k$ are considered as independent and white random variables, with normal probability distributions.

To perform the UKF technique, we also need to compose an augmented state vector $\mathbf{x}_k^a$ for unwrapping phase at the pixel with index k:

$$\mathbf{x}_k^a=\left[\mathbf{x}_k{}^T\quad \mathbf{v}_k{}^T\quad \mathbf{n}_k{}^T\right]^T. \tag{7}$$

Obviously, this augmented state vector is the direct concatenation of the original state vector, the process noise vector and the observation noise vector. Let the state vector covariance

#251481 Received 9 Oct 2015; revised 19 Nov 2015; accepted 19 Nov 2015; published 8 Dec 2015

matrix be $\mathbf{P}_x$, the process noise covariance matrix be $\mathbf{P}_v$ and the observation noise covariance matrix be $\mathbf{P}_n$. Then, the augmented state covariance matrix is built from

$$\mathbf{P}_k^a = \begin{bmatrix} \mathbf{P}_x & \mathbf{0} & \mathbf{0} \\ \mathbf{0} & \mathbf{P}_v & \mathbf{0} \\ \mathbf{0} & \mathbf{0} & \mathbf{P}_n \end{bmatrix}. \tag{8}$$

The proposed UKF-based phase unwrapping approach is presented in detail as follows, which is in the framework of the standard UKF technique.

- Initialize the UKF algorithm. We can choose a seed pixel ($k=1$) to start the UKF recursive estimation. The true phase of the seed pixel can be designated as the wrapped value simply. The augmented state covariance matrix for the seed pixel is a diagonal matrix whose elements are the initialized variances of the corresponding variables.

- Repeat the following steps (a)-(c) from $k=2$ to $k=end$, where, *end* is the pixel total number in a pixel sequence to be unwrapped:

(a) **Generate** the *sigma points*. The sigma points are a minimal set of carefully chosen samples that completely capture the true mean and covariance of a random variable. When the sigma points propagate through a non-linear system, the outputs can capture the posterior mean and covariance of this random variable accurately to the 3rd order (Taylor series expansion). The sigma points for the augmented state vector $\mathbf{x}_{k-1}^a$ are $2N+1$ vectors around its mean value, where, N is the dimension of the augmented state vector. We can form a sigma point matrix $\mathbf{X}_{k-1}^a$ whose i th column is the i th sigma point:

$$\mathbf{X}_{i,k-1}^a = \begin{cases} \mathbf{x}_{k-1}^a, & i=0, \\ \mathbf{x}_{k-1}^a + \left(\sqrt{(N+\lambda)\mathbf{P}_{k-1}^a}\right)_i, & i=1,...,N, \\ \mathbf{x}_{k-1}^a - \left(\sqrt{(N+\lambda)\mathbf{P}_{k-1}^a}\right)_i, & i=N+1,...,2N. \end{cases} \tag{9}$$

In Eq. (9), $\left(\sqrt{(N+\lambda)\mathbf{P}_{k-1}^a}\right)_i$ is the i th column of the matrix square root. $\lambda = \alpha^2(N+\kappa) - N$ is a scaling parameter, where, α and κ are tuning factors. Generally, κ is set to zero, and $0 \le \alpha \le 1$. The sigma point matrix can be partitioned as

$$\mathbf{X}_{i,k-1}^a = [\mathbf{X}_{i,k-1}^x \quad \mathbf{X}_{i,k-1}^v \quad \mathbf{X}_{i,k-1}^n]^T, \tag{10}$$

where, the superscript x, v, n mean the corresponding parts of the state vector, process noise vector and observation noise vector, respectively. We also need to calculate the corresponding weighting coefficients for every sigma vector:

$$\begin{aligned} W_0^{(m)} &= \lambda/(N+\lambda), \\ W_0^{(c)} &= \lambda/(N+\lambda) + (1-\alpha^2+\beta), \\ W_i^{(c)} &= W_i^{(m)} = 1/\{2(N+\lambda)\}, \quad i=1,...2N. \end{aligned} \tag{11}$$

#251481 Received 9 Oct 2015; revised 19 Nov 2015; accepted 19 Nov 2015; published 8 Dec 2015

where, β is used to incorporate prior knowledge of the distribution of the augmented state vector, and $\beta = 2$ is the optimal choice for Gaussian distribution.

(b) **Update** the state vector and observation vector for the next pixel to be unwrapped based on the current state vector, and estimate the updating mean and covariance through the sigma points. In this step, we should use the generated sigma points to determine the mean and covariance of the predicted state vector through the state-space model [Eq. (3)] as

$$\begin{aligned} &\mathbf{X}_{i,k|k-1}^{x} = f\left[\mathbf{X}_{i,k-1}^{x}, \mathbf{X}_{i,k-1}^{v}\right], i = 0,1,...,2N. \\ &\mathbf{x}_{k}^{-} = \sum_{i=0}^{2N} W_{i}^{(m)} \mathbf{X}_{i,k|k-1}^{x}, \\ &\mathbf{P}_{x_k}^{-} = \sum_{i=0}^{2N} W_{i}^{(c)} \left[\mathbf{X}_{i,k|k-1}^{x} - \mathbf{x}_{k}^{-}\right]\left[\mathbf{X}_{i,k|k-1}^{x} - \mathbf{x}_{k}^{-}\right]^{T}, \end{aligned} \tag{12}$$

Similarly, let the predicted sigma point $\mathbf{X}_{i,k|k-1}^{x}$ pass through the observation equation [Eq. (5)]. Then the observation vector $\mathbf{y}_{k}^{-}$ is also updated as

$$\begin{aligned} &\mathbf{y}_{i,k|k-1} = h\left[\mathbf{X}_{i,k|k-1}^{x}, \mathbf{X}_{i,k-1}^{n}\right], i = 0,1,...,2N, \\ &\mathbf{y}_{k}^{-} = \sum_{i=0}^{2N} W_{i}^{(m)} \mathbf{y}_{i,k|k-1}, \\ &\mathbf{P}_{y_k} = \sum_{i=0}^{2N} W_{i}^{(c)} \left[\mathbf{y}_{i,k|k-1} - \mathbf{y}_{k}^{-}\right]\left[\mathbf{y}_{i,k|k-1} - \mathbf{y}_{k}^{-}\right]^{T}. \end{aligned} \tag{13}$$

(c) **Correct** the estimation of the state vector. The last step is the correction for the updated state vector incorporating the measured data. In this step, the Kalman gain $\mathbf{K}_{k}$ is first calculated by

$$\begin{aligned} &\mathbf{P}_{x_k y_k} = \sum_{i=0}^{2N} W_{i}^{(c)} \left[\mathbf{X}_{i,k|k-1}^{x} - \mathbf{x}_{k}^{-}\right]\left[\mathbf{y}_{i,k|k-1} - \mathbf{y}_{k}^{-}\right]^{T}, \\ &\mathbf{K}_{k} = \mathbf{P}_{x_k y_k} \mathbf{P}_{y_k}^{-1}. \end{aligned} \tag{14}$$

Then correct the estimation of the state vector through the Kalman correction formula as

$$\mathbf{x}_{k} = \mathbf{x}_{k}^{-} + \mathbf{K}_{k}\left(\mathbf{y}_{k} - \mathbf{y}_{k}^{-}\right). \tag{15}$$

The unwrapped phase at the pixel k is just the first element of the obtained $\mathbf{x}_{k}$. At last, calculate the state vector covariance $\mathbf{P}_{x_k}$ after the correction in order to initiate the phase unwrapping for the next pixel by

$$\mathbf{P}_{x_k} = \mathbf{P}_{x_k}^{-} - \mathbf{K}_{k} \mathbf{P}_{y_k} \mathbf{K}_{k}^{T}. \tag{16}$$

To unwrap the whole phase map, we just need to carry out the above procedures recursively for all the pixel points, according to some unwrapping strategy.

2.2 Unwrapping strategy

From the above algorithm kernel, one can see that the proposed approach unwraps the phase of the next pixel based on the already unwrapped neighborhood phase and the measurement information. To initiate the phase unwrapping, we should choose a seed pixel and give an

#251481 Received 9 Oct 2015; revised 19 Nov 2015; accepted 19 Nov 2015; published 8 Dec 2015

arbitrary phase guess for it. Generally, we can directly adopt the wrapped phase of the seed pixel as its unwrapped value. Next, perform the phase unwrapping algorithm along a continuous pixel path. We will recommend two possible unwrapping strategies for the realization of the proposed algorithm in this subsection.

The first strategy is called *column-by-column unwrapping*, as illustrated in Fig. 1(a). The column that possesses the most number of effective pixels is chosen to be unwrapped firstly. For most realistic wrapped phase map, it has a circular effective pixel aperture. Thus, we can start unwrapping from the central column of the wrapped phase map. As illustrated in Fig. 1(a), the pixel A is chosen as the seed point, and perform the algorithm to estimate the state vectors for all the pixels in this column. Next, we unwrap the column that contains the pixel C. The state vector and covariance matrix already calculated for the pixel B should be used to initiate the unwrapping for this column so that the estimated phases between different columns are continuous. Similar unwrapping process can be made until the right half phase map is unwrapped. We emphasize again that when unwrapping the first pixel of each column, the state vector and covariance matrix of its unwrapped neighbor pixel should be chosen as the initiation values in the recursive processes, such as $C \equiv D$, $D \equiv E$, $F \equiv G$, $H \equiv I$, where, the notation "$\equiv$" means the initiation operation. After completing the unwrapping for the right half phase map, we can unwrap the left half one in the similar way. This unwrapping strategy is proper to be used when there exist no invalid areas in the wrapped phase map, and can be a good choice for most of the interferometric measurement applications.

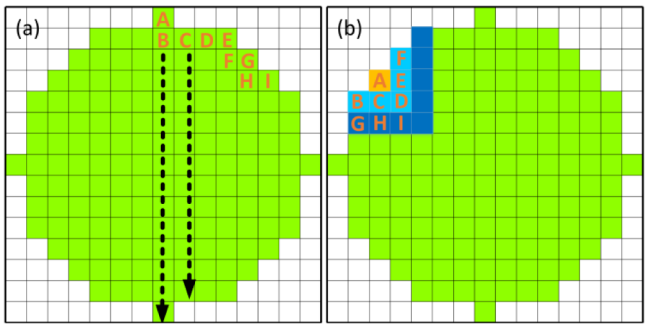

Fig. 1. Two recommended phase unwrapping strategies for the proposed algorithm: (a) column-by-column unwrapping and (b) the region growing unwrapping.

The second strategy we suggest to realize the proposed algorithm is the *region growing unwrapping* presented in Fig. 1(b). In this strategy, we should choose a pixel inside the valid wrapped phase map at random or in any prescribed order as the seed pixel, such as point A in Fig. 1(b). Then, establish a queue to store the pixel sequence to be unwrapped. When starting the phase unwrapping, push the adjacent wrapped pixels of A into the queue, such as the points $B \sim F$. Every time, we unwrap the headmost pixel in the queue; once a pixel is unwrapped, remove it from the queue, and push its wrapped neighbor pixels into the end of the queue. Repeat this process until all the pixels are unwrapped. In theory, this strategy is more universal for the proposed phase unwrapping algorithm, even when invalid areas such as holes occur in the original phase map. The region growing can bypass the invalid area according to the pre-determined phase mask so that the algorithm estimation would not be interrupted. The phase mask can be obtained commonly by some general imaging process methods combining the fringe modulation. We know that in the effective area of an interferogram, the modulation is remarkably large while the area with near zero modulation is considered as the useless parts such as holes and the outer boundary of images. Thus the modulations in the fringes would be a good metrics to discriminate the invalid areas, which can be easily calculated during the demodulation of phase-shift interferometers and spatial-carrier interferometers [2, 3].

#251481 Received 9 Oct 2015; revised 19 Nov 2015; accepted 19 Nov 2015; published 8 Dec 2015

3. Simulation validation

The proposed phase unwrapping algorithm is first validated through a simulated phase map with the size 256×256, which is generated by wrapping the peaks function in MATLAB, as shown in Fig. 2(a). Gauss white noise with the SNR of 15dB is added into the wrapped phase map in order to reveal the realistic condition. We employ the column-by-column unwrapping strategy simply in this validation. The covariance matrix for the vectors $\mathbf{v}_0$ is set to $diag([10^{-3}\ \ 10^{-4}])$, and that for the vector $\mathbf{n}_0$ is $diag([10^{-3}\ \ 10^{-3}])$. In fact, the performance of the proposed algorithm is not so sensitive to these initiation parameters. Generally, we can easily find proper values for them by several trials to guarantee successful unwrapping, and once determined, they are rather universal for many other utilities. In the following simulations and experiments, the values for these parameters are the same as that we have given herein if no other instructions are stated. After performing the proposed algorithm, the unwrapped phase is obtained, as shown in Fig. 2(b). We also present the unwrapping error in Fig. 2(c), which is the difference between the simulated true phase and the unwrapped one by the proposed algorithm. We can see that the peak-to-valley (PV) value and the root-mean-square (RMS) value of the unwrapping error are 1.29 rad and 0.16 rad respectively, demonstrating the feasibility and excellent phase unwrapping accuracy of the proposed algorithm.

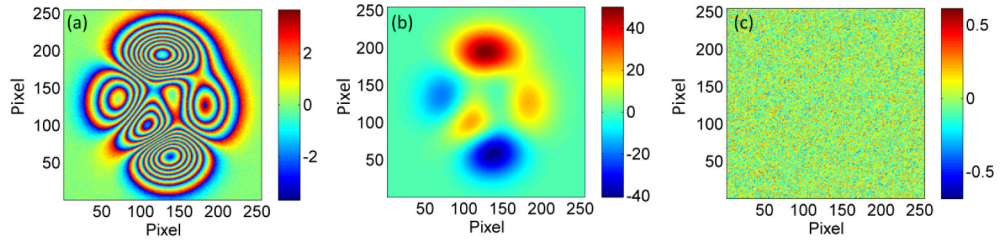

Fig. 2. Simulation validation of the proposed phase unwrapping algorithm: (a) the wrapped phase with the SNR of 15dB, (b) the unwrapped phase by the proposed algorithm, and (c) the phase unwrapping error. The unit of the phase is radian here.

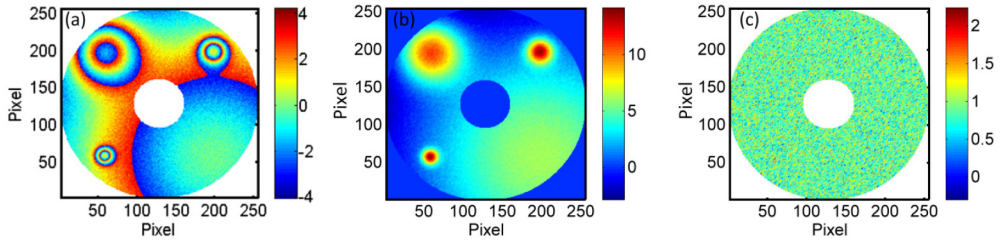

Fig. 3. Simulation validation of the proposed phase unwrapping algorithm: (a) the wrapped phase with the SNR of 10dB, (b) the unwrapped phase by the proposed algorithm, and (c) the phase unwrapping error. The unit of the phase is radian here.

The second simulation generates a phase function with Gauss peaks of different variation slopes distributed at the four corners of the phase map. At the phase center, a hole is introduced to simulate some interferometric application where we do not have a full-field phase map. Also, additive noise is introduced with a SNR of 10dB. The original wrapped phase map is presented in Fig. 3(a). To unwrap such a phase map, we use the suggested region growing strategy, and start the phase unwrapping from a random seed points in the valid area of the wrapped phase. Through the proposed algorithm, we obtain the unwrapped phase successfully, as shown in Fig. 3(b). The residual unwrapping error in Fig. 3(c) is with the PV value of 3.02 rad and RMS value of 0.25 rad. From this simulation, we can find that

#251481 Received 9 Oct 2015; revised 19 Nov 2015; accepted 19 Nov 2015; published 8 Dec 2015

the proposed algorithm is still stable when processing the wrapped phase that has invalid area, and keeps high accuracy even when the phase noise is large.

To compare the performance of the proposed algorithm with some commonly used phase unwrapping approaches, we unwrap a phase map similar to that in Fig. 2 but with lower SNR of 5dB. The original phase map with size 256×256 and the noise-corrupted wrapped one are presented in Figs. 4(a) and 4(b), respectively. We choose four typical phase unwrapping algorithms, each corresponding to one of the three algorithm categories introduced in Section 1, to perform the unwrapping together, and compare their results with that of the proposed one. The chosen four algorithms are the discrete cosine transform based least-squares (DCT-LS) method [11], the quality-guided path-following (QG-PF) method [9], the RPU method [14–16], and the RPT method [12]. Note that, the SNR of 5dB seems to be quite low which would be rare in real interferometric measurements. Testing the performance of these algorithms in such a limiting case is beneficial to study their characteristics sufficiently. It should be pointed out that, the RPT, with the steepest-descent method, has four degrees of freedom, i.e., the regularization parameter λ, the size of the neighborhood Γ, and the step size μ of the steepest-descent method. To reach the highest performance of the RPT, we made many trials to optimize the parameters determination for it, and the ultimate choices are: $\lambda=4$, $\Gamma=7$ and $\mu=0.001$. The RPU has one parameter τ that needs to be given first. In this phase unwrapping, we found $\tau=0.8$ is optimal for the RPU. At the same time, we also changed the covariance matrix for the vectors $\mathbf{v}_0$ to $diag([10^{-2.5}\quad 10^{-2.5}])$, and that for the vector $\mathbf{n}_0$ to $diag([10^{-1}\quad 10^{-1}])$ as for the proposed algorithm.

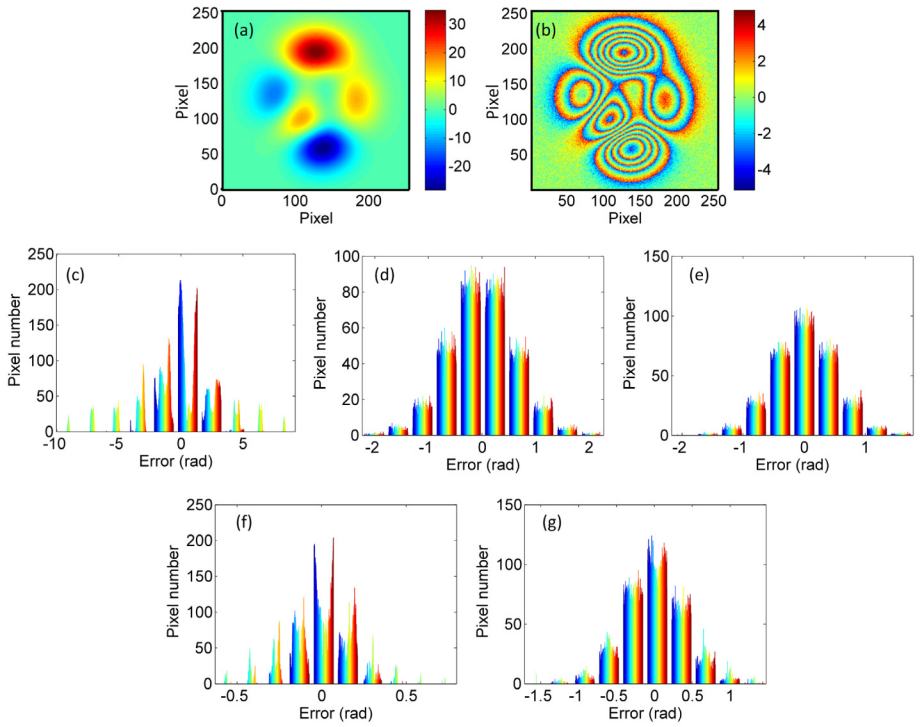

Fig. 4. Performance comparisons between several typical phase unwrapping algorithms. (a) is the simulated original phase map, (b) is the noise-corrupted wrapped phase map with SNR of 5dB, (c)-(g) are the histograms of residual unwrapping errors by the DCT-LS, the QG-PF, the RPU, the RPT, and the proposed algorithm, respectively. The unit of the phase is radian here.

#251481 Received 9 Oct 2015; revised 19 Nov 2015; accepted 19 Nov 2015; published 8 Dec 2015

Figures 4(c)-4(g) show the histograms of unwrapping errors through the DCT-LS, the QG-PF, the RPU, the RPT, and the proposed algorithm, respectively. The details for these results are given in Table 1. All these simulations are conducted through MATLAB R2014 in a computer with the Intel i3 processer of 3.5 GHz. From Fig. 4 and Table 1, it is noticeable that the performance of the DCT-LS method is not comparable to other algorithms in this high noise situation, although it is very fast. The RPU outperforms the QG-PF in both the algorithm accuracy and speed. Our proposed approach has smaller unwrapping error than that of the RPU, while its time consumption is a little more than that of the RPU. Moreover, it is noteworthy that the RPT approach has the best accuracy while it needs far more processing time than other algorithms (more than 20 times that of our approach, for example). Obviously, it is the result of excessively recursive searching in the RPT process in order to minimize the cost function. Considering the algorithm accuracy and speed comprehensively, our approach and the RPU are no doubt the very practical choices for the phase unwrapping of interferometric fringes.

Table 1. Details of the phase unwrapping accuracy and time consumption through different algorithms.

Algorithm	DCT-LS	QG-PF	RPU	RPT	proposed
PV/rad	19.26	4.51	3.95	1.43	3.19
RMS/rad	2.59	0.56	0.46	0.16	0.34
Time/s	0.3	67.2	2.5	242.5	11.9

The DCT-LS method has the worst unwrapping accuracy in this case because it reduces the dynamic ranges of the true phase map in the serious noise condition, which is a drawback of the least-squares method in the phase unwrapping application, as already known in this realm. The accuracy of the QG-PF method is intermediate among these algorithms due to its lack of noise filtering ability. The RPU can filter out the noise to some extent during the unwrapping process because of the essence of infinite impulse response (IIR) low-pass filter. The noise suppression abilities of the RPT and the proposed algorithm are much more obvious from the smaller error PVs and RMSs than other approaches. As is known, to obtain good noise filtering, we should choose a relatively large neighborhood size for the RPT. In this case, the iteration times for unwrapping each pixel are also enlarged in order to minimize the cost function to an acceptable level (generally, 20~30 iterations are needed to unwrap one pixel). Thus, the RPT has very remarkable noise filtering capacity but at the cost of very high computation consumption. Although the proposed algorithm unwraps one pixel just through one-step prediction and one-step correction, it can also resist the phase noise quite well. This should attribute to the optimal estimation characteristic of the UKF technique. Therefore, our algorithm can provide satisfactory accuracy even in the severe noise situation while using relatively low time cost. It is interesting to note that the RPU can also be considered as a predictor-corrector model [15]. However, comparing to the proposed algorithm, the RPU cannot give the optimal data fusion of the prediction and observation. This may be the reason why our algorithm has better accuracy and noise suppression capacity than the RPU.

Based on these simulation validations, we are confident that the proposed approach is very practical for the phase unwrapping of interferometric fringes considering the high accuracy, good noise suppression and low computation cost.

4. Experimental test

In this section, we will give some real application examples of the proposed phase unwrapping algorithm to demonstrate its feasibility and capacity. These examples stem from different optical interferometer systems developed by our team. In fact, the proposed approach has been an important part in the data analysis software of our interferometer instruments recently.

#251481 Received 9 Oct 2015; revised 19 Nov 2015; accepted 19 Nov 2015; published 8 Dec 2015

Figure 5 illustrates the application of the proposed algorithm in the field-widened Michelson interferometer (FWMI) characterization experiment. We are developing an FWMI to act as a spectral filter in a high-spectral-resolution lidar (HSRL) instrument [26]. In the process of FWMI establishment, we need to estimate the field-widening characteristic of the interferometer. The interferogram during the FWMI optimization is the circular fringes as presented in Fig. 5(a). A simple 4-step phase-shifting demodulation algorithm is employed to retrieve the phase variation corresponding to Fig. 5(a). The wrapped phase map after the 4-step phase-shifting demodulation is shown in Fig. 5(b), and after phase unwrapping by the proposed algorithm, the continuous phase map is obtained shown in Fig. 5(c). The unwrapping result seems to be very good, although we cannot know the true phase value to estimate the unwrapping error, as done in the simulation section. However, since the accuracy and noise suppression ability of the algorithm have already been demonstrated sufficiently in Section 3, we believe that the unwrapped phase here is rather accurate.

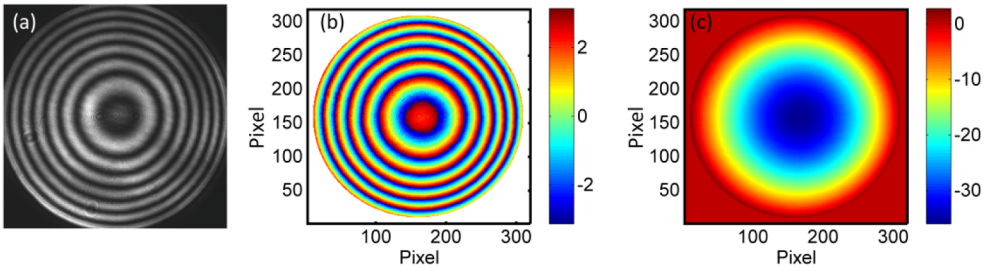

Fig. 5. The application of the proposed algorithm in the field-widened Michelson interferometer system. (a) one of the original interferogram for the 4-step phase-shifting demodulation, (b) the wrapped phase map after the 4-step phase-shifting demodulation, and (c) the unwrapped phase map through the proposed method. The unit of the phase is radian here.

Figure 6 gives the application example of the proposed phase unwrapping algorithm in our developed point diffraction interferometry (PDI) for spherical surfaces measurement [27, 28]. The interferogram in this interferometer contains straight fringes, as shown in Fig. 6(a). It also employs the phase-shifting technique to modulate the testing wavefront carrying the surface figure information, which interferes with the pinhole diffraction reference wavefront. After demodulating by the phase-shifting method, the wrapped phase is presented in Fig. 6(b). Performing the phase unwrapping through the proposed algorithm, we get the unwrapped phase successfully as given in Fig. 6(c). The unwrapped phase map lays the foundation for subsequent data processing such as eliminating the constant term and tilt term in the phase map using the Zernike polynomial decomposition in order to obtain the ultimate tested surface figure.

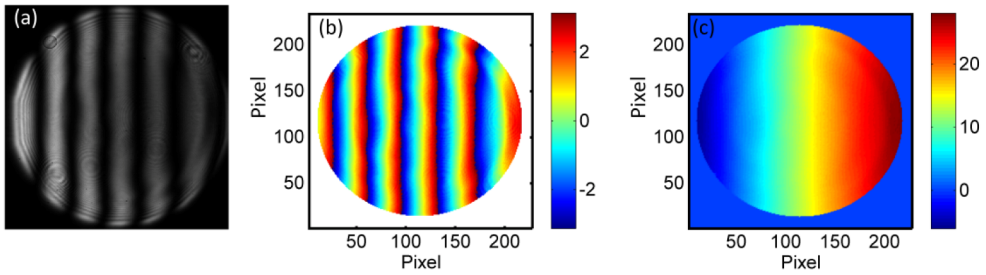

Fig. 6. The application of the proposed algorithm in the phase-shift point diffraction interferometer system. (a) one of the original interferogram for the phase-shifting demodulation, (b) the wrapped phase map after demodulation, and (c) the unwrapped phase map through the proposed method. The unit of the phase is radian here.

#251481 Received 9 Oct 2015; revised 19 Nov 2015; accepted 19 Nov 2015; published 8 Dec 2015

The proposed phase unwrapping algorithm is also verified in an off-axis cyclic radial shearing interferometer (OCRSI) which is also developed by our team to measure centrally blocked transient wavefront [29], for example, in transient measurement of hypersonic flow field with a model in a wind tunnel. The OCRSI adopts the spatial carrier technique and Fourier transform method to retrieve the tested wavefront [2]. Figure 7(a) shows the typical interferogram the OCRSI formed, and the wrapped wavefront map is presented in Fig. 7(b) through the Fourier transform demodulation. From Figs. 7(a) and 7(b), we can see clearly that the center part of the aperture is blocked. The unwrapped phase via the proposed algorithm is shown in Fig. 7(c), where, the phase unwrapping is also very successful.

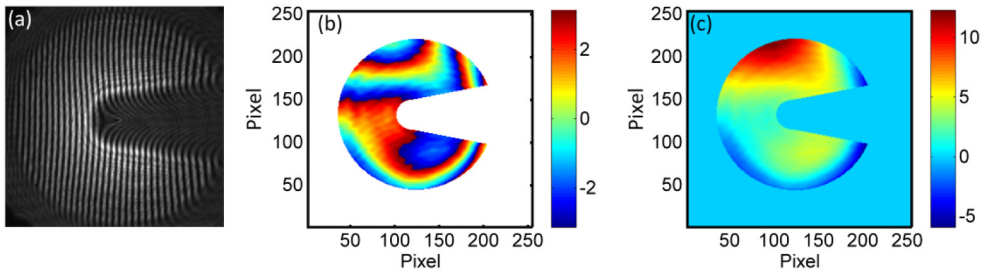

Fig. 7. The application of the proposed algorithm in the off-axis cyclic radial shearing interferometer system. (a) the original spatial carrier interferogram, (b) the wrapped phase map after the Fourier transform demodulation, and (c) the unwrapped phase map through the proposed method. The unit of the phase is radian here.

To test the practical performance of the algorithm further, we would like to unwrap a more complicated phase map here. Figure 8(a) shows one of phase-shifting interferograms generated intentionally via our non-null annular sub-aperture stitching interferometry (NASSI) for steep aspheric and free-form surface measurement [1]. Note that, such interferograms are in fact very rare in the normal usage of NASSI system. We just produce these special fringes to verify the algorithm robustness. The wrapped phase map is shown in Fig. 8(b) through the phase-shifting demodulation. After performing the proposed algorithm, the unwrapped phase can be obtained successfully which is shown in Fig. 8(c).

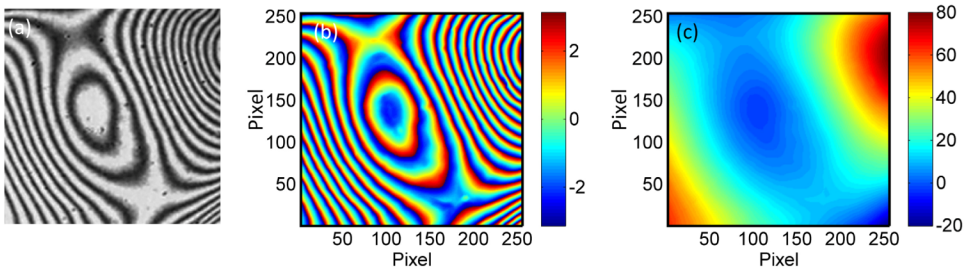

Fig. 8. The application of the proposed algorithm for unwrapping a complicated phase map generated in the non-null annular sub-aperture stitching interferometry. (a) one of the original interferogram for the phase-shifting demodulation, (b) the wrapped phase map after demodulation, and (c) the unwrapped phase map through the proposed method. The unit of the phase is radian here.

5. Conclusion

A phase unwrapping algorithm based on unscented Kalman filter technique is proposed which is intended for applications in the interferometric measurements, such as the wavefront testing, surface figure testing of optics, etc. Two unwrapping strategies for the proposed algorithm are introduced, i.e., column-by-column unwrapping and region growing unwrapping. We tested the performance of the proposed algorithm by simulations with

#251481 Received 9 Oct 2015; revised 19 Nov 2015; accepted 19 Nov 2015; published 8 Dec 2015

different phase maps incorporating different levels of noise and good unwrapping accuracy is verified. We also compare its performance with some most used phase unwrapping approaches such as the DCT-LS method, the QG-PF method, the RPU method, and the RPT method. Results demonstrate the satisfactory accuracy and noise filtering characteristic of the proposed one. Also, the time consumption of the algorithm is reasonably acceptable. The algorithm has already been used in our different interferometer systems, such as the FWMI, the PDI, and the OCRSI, successfully, and very good performance is obtained. We hope that this algorithm can be a practical solution for the phase unwrapping of interferometric fringes to enhance the measurement accuracy.

Acknowledgment

This work was partially supported by the National Natural Science Foundation of China (NSFC) (41305014, 11275172, 61475141), the Specialized Research Fund for the Doctoral Program of Higher Education of China (20130101120133), the Aviation Science Funds (20140376001), the Fundamental Research Funds for the Central Universities (2013QNA5006), the State Key Lab. of Modern Optical Instrumentation Innovation Program (MOI2015QN01), the State Key Laboratory of Applied Optics.

#251481 Received 9 Oct 2015; revised 19 Nov 2015; accepted 19 Nov 2015; published 8 Dec 2015